VI

Neutrinos

When the Standard Model first emerged, there was no evidence of neutrino mass. Since only left-chiral neutrino fields are coupled to the gauge bosons, the simplest way to accommodate the lack of a neutrino mass was to omit any right-handed counterparts to the neutrino field, in which case masslessness is automatic. Because of the degeneracy of the three massless neutrinos, the charged weak leptonic current can be made diagonal and there exists no lepton analog to the CKM matrix.

In light of evidence for neutrino mass, the most conservative response is to postulate the existence of right-handed neutrinos, similar to the right-handed partners of the other fields. Because the right-handed neutrino carries no gauge charge, its mass may be Dirac or Majorana (or both), and it may be heavy or light. Whether one considers this modification to be an extension beyond the Standard Model or not is largely a matter of semantics. In this chapter, we will describe the rich physics induced by the inclusion of a right-handed neutrino. We note in passing that all fermion fields appearing here will be described as four-component spinors.

VI–1 Neutrino mass

A right-handed neutrino ν_R has no couplings to any of the gauge fields because its Standard Model charges are zero.[1] Nonetheless, it can enter the lagrangian in two ways: there can be a Yukawa coupling to lepton doublet ℓ_L plus a Higgs and there can be a Majorana mass term involving ν_R. Considering only one generation for the moment, these possibilities are[2]

$$\mathcal{L}_{\nu_R} = -g_\nu \overline{\ell}_L \widetilde{\Phi} \nu_R - \frac{m_M}{2} \overline{(\nu_R)^c}\, \nu_R \;+\; \text{h.c.} \tag{1.1}$$

[1] ν_R is electrically neutral ($Q = 0$) and like all RH particles in the Standard Model is a weak isosinglet ($T_{\text{w}3} = 0$), so by Eq. (II–3.8) it has zero weak hypercharge, $Y_{\text{w}} = 0$.

[2] In neutrino physics, a *sterile neutrino* is defined as one which has no interactions whatsoever with Standard Model particles. The right-handed neutrino discussed here is *not* sterile if $g_\nu \neq 0$ because it can then couple to the Higgs field as in Eq. (1.1).

https://doi.org/10.1017/9781009291033.007 Published online by Cambridge University Press

Recall that the left-handed neutrino field is part of an $SU(2)_L$ doublet and so can have no Majorana mass term because the combination $\overline{(\nu_L)^c}\ \nu_L$ is not gauge-invariant. The right-handed Majorana mass could be set equal to zero by the imposition of a discrete symmetry (e.g. lepton number) but this is an additional assumption beyond the Standard Model gauge symmetries.

When the Higgs field picks up a vacuum expectation value, this leads to a mass matrix of the form

$$-2\,\mathcal{L}_{D+M} = \left(\overline{\nu_L}\ \ \overline{(\nu_R)^c}\right)\begin{pmatrix} 0 & m_D \\ m_D & m_M \end{pmatrix}\begin{pmatrix} \nu_L^c \\ \nu_R \end{pmatrix} + \text{h.c.}, \tag{1.2}$$

where the Dirac mass is $m_D = g_\nu v/\sqrt{2}$ and where we have used the fact that $\overline{(\psi_i)^c}\psi_j^c = \overline{(\psi_j)}\psi_i$. The above matrix can be diagonalized by defining fields

$$\nu_a = \cos\theta\ \nu_R + \sin\theta\ \nu_L^c\ , \qquad \nu_b = \cos\theta\ \nu_L - \sin\theta\ \nu_R^c, \tag{1.3}$$

with $\tan 2\theta = 2m_D/m_M$. The mass terms then become

$$-\mathcal{L}_{D+M} = \frac{m_a}{2}\left[\overline{(\nu_a)^c}\nu_a + \overline{(\nu_a)}\nu_a^c\right] + \frac{m_b}{2}\left[\overline{(\nu_b)^c}\nu_b + \overline{(\nu_b)}\nu_b^c\right], \tag{1.4}$$

with

$$m_a = m_M\cos^2\theta + m_D\sin 2\theta\ , \qquad m_b = m_M\sin^2\theta - m_D\sin 2\theta. \tag{1.5}$$

The mass matrix of Eq. (1.2) has one negative eigenvalue, and given the mixing angle this can be seen to be m_b. As discussed earlier in Sect. I–3, this is kinematically equivalent to a positive mass, and the eigenvalue can be made positive by the phase change $\nu_b \to i\,\nu_b$. However, we shall leave the phase unchanged as it would induce an unusual phase in the weak mixing matrix. Finally, inverting Eq. (1.3) yields the following relation between the neutrino field ν_L and the mass eigenstates ν_a^c and ν_b,

$$\nu_L = \cos\theta\ \nu_b + \sin\theta\ \nu_a^c. \tag{1.6}$$

It is this combination of the mass eigenstates which constitutes the neutrino component of charged and neutral weak currents first encountered in Sect. II–3.

There are two obvious limiting cases for the mass matrix of Eq. (1.2). In one limit, the Majorana mass term vanishes, $m_M = 0$, with the result that the neutrino is a Dirac fermion with mass m_D. Here, both particle and antiparticle can have positive helicity (right-handed) or negative helicity (left-handed), so there are four degrees of freedom. As noted in Sect. I–3, despite appearances, Eq. (1.4) reduces to the standard Dirac lagrangian in this limit (with $\theta = \pi/4$ and $m_a = -m_b = m_D$).

https://doi.org/10.1017/9781009291033.007 Published online by Cambridge University Press

The other case is that of a very large Majorana mass m_M. Here, one eigenvalue becomes large and the other small,

$$m_a = m_M \ , \qquad m_b = -\frac{m_D^2}{m_M}. \tag{1.7}$$

The mixing angle in this case becomes tiny, $\theta = m_D/m_M \ll 1$, so that eigenfunctions are just $\nu_a = \nu_R$, $\nu_b = \nu_L$ up to corrections of order $m_{\rm D}/m_{\rm M}$. Both of these eigenstates are Majorana fields.[3] There are still four degrees of freedom present, viz. left-handed and right-handed helicity states for each of the two self-conjugate neutrinos. This is the famous *seesaw mechanism* [GeRS 79], which has the potential to explain the fact that the neutrinos are much lighter than the quarks and other leptons. As an example, given the mass constraints cited in Chap. I, at least one neutrino must have rest-energy in excess of 0.05 eV, and if we use m_τ for the corresponding Dirac mass, this would be compatible with $m_M \sim 6\times 10^{10}$ GeV. We see that the light field in this case is a Majorana field of the left-handed neutrino. Even though the direct left-handed Majorana mass term was forbidden by gauge symmetry, after symmetry breaking the left-handed field assumes a Majorana nature. We can understand this feature more directly using effective lagrangian techniques, to which we now turn.

Equivalence of heavy Majorana mass to a dimension-five operator

We have explained in Chap. IV how a heavy field may be integrated out from a theory. Here, we consider a process that involves two applications of the first term in Eq. (1.1), $g_\nu \overline{\ell}_L \widetilde{\Phi} \nu_R$, in which the right-handed neutrino is a (self-conjugate!) Majorana fermion. If the Majorana mass is large, ν_R becomes heavy and can accordingly be removed. We then find the following residual interaction [We 79a] involving just the light fields,

$$\mathcal{L}_5 = -\frac{1}{\Lambda_M} \overline{\ell}_L \widetilde{\Phi} \widetilde{\Phi} \ell_L^c \ + \ \text{h.c.}, \tag{1.8}$$

where $1/\Lambda_M \equiv g_\nu^2/(2m_M)$. This interaction is invariant under $SU(2)_L$ gauge interactions because the lepton doublet and the Higgs doublet both transform in the same way. The fields in $\mathcal{L}_5$ carry a total mass dimension of five. Hence, this operator must have a coupling constant with the dimensions of an inverse mass, and so the operator cannot be part of a renormalizable lagrangian. However, in effective field theory, this operator *is* an allowed addition to the lagrangian of the light Standard Model fields, and it is suppressed by a single power of the heavy scale m_M.

[3] In the general case, where the mass parameters m_a, m_b are allowed to have arbitrary values, both neutrinos are Majorana. In fact, a Dirac neutrino can itself be interpreted as a pair of degenerate Majorana neutrinos.

https://doi.org/10.1017/9781009291033.007 Published online by Cambridge University Press

Once the Higgs field picks up its vacuum expectation value, this lagrangian turns into a Majorana lagrangian for the left-handed neutrino,

$$\mathcal{L}_5 \to -\frac{v^2}{2\Lambda_M}\overline{\nu}_L \nu_L^c \; + \; \text{h.c.}, \tag{1.9}$$

reproducing the mass eigenvalue and eigenfunction calculated above via diagonalization. So we see that a left-handed Majorana mass term *is* allowed after the electroweak symmetry breaking if we include operators of dimension five. Indeed, although we have just found the above operator by integrating out a particular heavy field, its existence can be more general than this particular calculation. There could be other theories beyond the Standard Model which might generate this operator.

The properties of neutrino mass are suggestive of physics beyond the Standard Model, although they are not conclusive proof of that. We have seen that there is no conflict between the idea of neutrino mass and the symmetries of the Standard Model. Once one allows the possibility of right-handed neutrino fields, both Dirac and Majorana mass terms will occur unless one makes an additional symmetry assumption of lepton-number conservation, which would set the Majorana mass equal to zero. Even if this extra discrete symmetry were imposed, Dirac masses could still account for observations. However, the small magnitude of the observed neutrino masses is puzzling in one way or another. If the Majorana masses are small or zero such that Dirac masses are dominant, one would require the Yukawa couplings to be remarkably small – roughly a billion times smaller than the Yukawas for the charged leptons. On the other hand, if the Majorana mass is large, the neutrino masses are naturally small via the seesaw mechanism, but then one has to understand the large value of the Majorana scale. A Majorana mass in the range $10^6 \to 10^{14}$ GeV would not match any of the scales of the Standard Model (nor does it match estimates of Grand Unification scales). While the present structure is consistent with the interactions of the Standard Model, we hope that future New Physics will explain the puzzles of the quark and lepton mass scales, which are most dramatic in the case of neutrino masses.

VI–2 Lepton mixing

In the previous section we considered mass diagonalization for a single species of neutrino. In the Standard Model, there are, however, three generations of leptons. This means that both the Dirac and Majorana mass terms will involve 3×3 matrices, $\mathbf{m}_D$ and $\mathbf{m}_M$. The Dirac mass matrix is, in general, complex but not Hermitian, while the Majorana mass matrix will be complex symmetric. The overall mass matrix must be diagonalized, and there will be a resultant weak mixing matrix

https://doi.org/10.1017/9781009291033.007 Published online by Cambridge University Press

for the charged weak current. We shall consider lepton mixing in the two limiting cases discussed above, first for a pure Dirac neutrino mass and then in the seesaw limit.

Dirac mass: The biunitary diagonalization of the lepton mass matrices has already been carried out in Eqs. (II–4.1)–(II–4.7b) for the case of a pure Dirac mass. The results for leptons proceed analogously to those for quarks. Mixing between generations occurs in the leptonic charged weak current (recall that the lepton mass eigenstates are $\vec{\nu}_L = \{\nu_1, \nu_2, \nu_3\}_L$ and $\vec{e}_L = \{e, \mu, \tau\}_L$),

$$J^{\mu}_{\rm ch}(\text{lept}) = 2\vec{\overline{\nu}}'_L \gamma^{\mu} \vec{e}'_L = 2\vec{\overline{\nu}}_L \mathbf{S}^{\nu\dagger}_L \mathbf{S}^{e}_L \gamma^{\mu} \vec{e}_L \equiv 2\vec{\overline{\nu}}_L \mathbf{V}^{(\nu)} \gamma^{\mu} \vec{e}_L, \tag{2.1}$$

where

$$\mathbf{V}^{(\nu)} \equiv \mathbf{S}^{\nu\dagger}_L \mathbf{S}^{e}_L \tag{2.2}$$

is the Dirac lepton mixing matrix. As an example, the electron's contribution to the charged weak current is given by

$$J^{\mu}_{\rm ch}(\text{e}) = 2[\bar{\nu}_{L,1}\mathbf{V}^{(\nu)}_{1e} + \bar{\nu}_{L,2}\mathbf{V}^{(\nu)}_{2e} + \bar{\nu}_{L,3}\mathbf{V}^{(\nu)}_{3e}]\gamma^{\mu} e_L \equiv 2\overline{\nu}_{L,e}\gamma^{\mu} e_L, \tag{2.3}$$

which shows the neutrino $\nu_{L,e}$ created in this process to be a linear combination of the three neutrino mass eigenstates. The lepton mixing matrix $\mathbf{V}^{(\nu)}$ of Eq. (2.2) will have the same structure as the quark mixing matrix of Eq. (II–4.17) with three mixing angles $\{\theta_{ij}\}$ and one *CP*-violating phase δ.

Majorana mass: If the right-handed Majorana mass is very large, or if we invoke the dimension-five operator of the previous section, we see that the light eigenstate is a left-handed Majorana particle with mass

$$\mathbf{m}_L = -\mathbf{m}_D \frac{1}{\mathbf{m}_M} \mathbf{m}^T_D. \tag{2.4}$$

Here, the factors are themselves 3×3 matrices and we have been careful with the ordering of the elements.

The matrix $\mathbf{m}_L$ is nondiagonal, as are the individual elements $\mathbf{m}_D$ and $\mathbf{m}_M$. The Dirac part is diagonalized as

$$\mathbf{m}^{(\text{diag})}_D = \mathbf{S}^{\nu\dagger}_L \mathbf{m}_D \mathbf{S}^{\nu}_R. \tag{2.5}$$

Inserting the diagonalized Dirac part into the full mass matrix yields

$$\mathbf{m}_L = \mathbf{S}^{\nu}_L \, \mathcal{C} \, \mathbf{S}^{\nu T}_L, \tag{2.6}$$

where the central matrix $\mathcal{C}$ is defined as

$$\mathcal{C} \equiv \mathbf{m}^{(\text{diag})}_D \mathbf{S}^{\nu\dagger}_R \frac{1}{\mathbf{m}_M} \mathbf{S}^{\nu *}_R \mathbf{m}^{(\text{diag})}_D. \tag{2.7}$$

https://doi.org/10.1017/9781009291033.007 Published online by Cambridge University Press

The symmetric (but generally complex-valued) central matrix $\mathcal{C}$ can be diagonalized with a unitary matrix $\mathcal{F}$,

$$\mathcal{C} = \mathcal{F}\,\mathbf{m}_\nu\,\mathcal{F}^T = \mathcal{F}\begin{pmatrix} m_1 & 0 & 0 \\ 0 & m_2 & 0 \\ 0 & 0 & m_3 \end{pmatrix}\mathcal{F}^T. \tag{2.8}$$

The masses in the diagonal matrix $\mathbf{m}_\nu$ are the physical neutrino masses.

The PMNS matrix involves the rotations that diagonalize the mass matrices of the charged leptons and the neutrinos [Po 68, MaNS 62]. This also includes the rotation that diagonalizes the central matrix. Therefore, in terms of the quantities defined above, the PMNS matrix becomes

$$\mathbf{U} = \mathcal{F}^\dagger \mathbf{S}_L^{\nu\dagger} \mathbf{S}_L^e. \tag{2.9}$$

Like the $n \times n$ Dirac mixing matrix for quarks and leptons, the Majorana mixing matrix has n^2 real-valued parameters, of which $n(n-1)/2$ are angles and $n(n+1)/2$ are phases. However, whereas field redefinitions remove $2n-1$ phases for the Dirac case, only n such phases can be removed (via redefinitions of the charged lepton fields) for the Majorana mixing matrix. The reason is that Majorana fields are self-conjugate (cf. Sect. I–3) and thus not subject to phase redefinitions.[4] Thus, the number of remaining phases in the Majorana mixing matrix is $n(n-1)/2$. For $n = 3$ there are three phases, of which one is identified as the phase δ in the Dirac mixing matrix and two others, α_1, α_2, are commonly called Majorana phases. It can be shown that

$$\mathbf{U} = \mathbf{V}^{(\nu)}\mathcal{P}_\nu \quad \text{with} \quad \mathcal{P}_\nu = \begin{pmatrix} 1 & 0 & 0 \\ 0 & e^{i\alpha_1/2} & 0 \\ 0 & 0 & e^{i\alpha_2/2} \end{pmatrix}, \tag{2.10}$$

where the $\{\alpha_i\}$ are the Majorana phases. For convenience, we give the neutrino mixing matrix $\mathbf{V}^{(\nu)}$,

$$\mathbf{V}^{(\nu)} = \begin{pmatrix} c_{12}c_{13} & s_{12}c_{13} & s_{13}e^{-i\delta} \\ -s_{12}c_{23} - c_{12}s_{23}s_{13}e^{i\delta} & c_{12}c_{23} - s_{12}s_{23}s_{13}e^{i\delta} & s_{23}c_{13} \\ s_{12}s_{23} - c_{12}c_{23}s_{13}e^{i\delta} & -s_{23}c_{12} - s_{12}c_{23}s_{13}e^{i\delta} & c_{23}c_{13} \end{pmatrix}, \tag{2.11}$$

where $s_{\alpha\beta} \equiv \sin\theta_{\alpha\beta}$, $c_{\alpha\beta} \equiv \cos\theta_{\alpha\beta}$ $(\alpha, \beta = 1, 2, 3)$.

[4] If $\psi \to e^{i\theta}\psi$, then $(\psi)^c \to e^{-i\theta}(\psi)^c$. Maintaining the Majorana condition $\psi = \psi^c$ occurs only for $\theta_n = n\pi$, so θ cannot be arbitrary.

https://doi.org/10.1017/9781009291033.007 Published online by Cambridge University Press

VI–3 Theory of neutrino oscillations

Our current information on neutrino mass and mixing comes via the phenomenon of neutrino oscillations. We review the foundation of this subject in the present section.

Oscillations in vacuum

Suppose that at time $t = 0$ an electron neutrino is produced by a weak process induced by the charged current $J^{\mu}_{\rm ch}(e)$ of Eq. (2.3) and thereafter propagates as an eigenstate of momentum $\mathbf{p}$,

$$|\nu_e(0)\rangle \to |\nu_e(t)\rangle = U^*_{e1}|\nu_1\rangle e^{-iE_1 t} + U^*_{e2}|\nu_2\rangle e^{-iE_2 t} + U^*_{e3}|\nu_3\rangle e^{-iE_3 t}, \qquad (3.1)$$

where $E_i = (\mathbf{p}^2 + m_i^2)^{1/2}$. In this relation, the mixing matrix elements $\{U_{ek}\}$ $(k = 1, 2, 3)$ appear as complex conjugates because the neutrino field in the charged current is in the form of a Hermitian conjugate $\overline{\nu}_e$. Actually, as written Eq. (3.1) is theoretically tainted because the superposition cannot be a simultaneous eigenstate of both momentum and energy since $m_1 \neq m_2 \neq m_3$. However, since this simplified description leads to the correct oscillation phase under rather general conditions, we continue to use it here.[5]

To proceed, we take $p \gg m_i$, implying that $E_i \simeq p + m_i^2/(2p) \simeq p + m_i^2/(2E)$. Upon replacing the time by the distance traveled, $t \simeq L$, we obtain from Eq. (3.1),

$$|\nu_e(L)\rangle \simeq e^{-iE_1 L}\left(U^*_{e1}|\nu_1\rangle + U^*_{e2}|\nu_2\rangle \exp\left[-i\frac{m_2^2 - m_1^2}{2E}L\right] + U^*_{e3}|\nu_3\rangle \exp\left[-i\frac{m_3^2 - m_1^2}{2E}L\right]\right). \qquad (3.2)$$

Let us now truncate the description to just two neutrino flavors by working in the small θ_{13} limit, evidently a reasonable approximation given that $|U_{e3}/U_{e1}| \simeq 0.16$.

Then, the amplitude $\mathcal{A}_{\nu_e\nu_e}(L)$ and probability $\mathcal{P}_{\nu_e\nu_e}(L)$ for remaining in the original weak eigenstate $\nu_e(0)$ at distance L become

$$\mathcal{A}_{\nu_e\nu_e}(L) = \langle\nu_e(0)|\nu_e(L)\rangle = e^{-iE_1 L}\left(|U_{e1}|^2 + |U_{e2}|^2 \exp\left[-i\frac{m_2^2 - m_1^2}{2E}L\right]\right)$$
$$\mathcal{P}_{\nu_e\nu_e}(L) = |\mathcal{A}_{\nu_e\nu_e}(L)|^2 = c_{12}^4 + s_{12}^4 + 2c_{12}^2 s_{12}^2 \cos\left[\frac{\Delta m_{21}^2}{2E}L\right]. \qquad (3.3)$$

[5] Two recent discussions of this point appear in [KaKRV 10] and [CoGL 09], but many others have contributed to the topic. See references cited in [GiK 07] and [RPP 12].

https://doi.org/10.1017/9781009291033.007 Published online by Cambridge University Press

With a bit of algebra, we then obtain for the survival and transition probabilities $\mathcal{P}_{\nu_e\nu_e}(L)$ and $\mathcal{P}_{\nu_e\nu_\mu}(L)$,

$$\mathcal{P}_{\nu_e\nu_e}(L) = 1 - \sin^2 2\theta_{12}\ \sin^2\left[\frac{\Delta m^2_{21} L}{4E}\right],$$
$$\mathcal{P}_{\nu_e\nu_\mu}(L) = \sin^2 2\theta_{12} \sin^2\left[\frac{\Delta m^2_{21} L}{4E}\right]. \tag{3.4a}$$

Let us comment on aspects of these important relations. The amplitude of the oscillation factor is $\sin^2 2\theta_{12}$. The oscillation phase $\Phi_{21} \equiv \Delta m^2_{21} L/(4E)$ informs about the squared mass-difference Δm^2_{21}, given that the energy (E) and distance (L) are dictated by constraints of Nature and/or by experimental design.[6] An expression useful for numerical work is

$$\Phi_{21} \simeq 1.267\ \frac{\Delta m^2_{21}[\mathrm{eV}^2]\ L[m]}{E[\mathrm{MeV}]}. \tag{3.4b}$$

Another involves defining an oscillation *length* $L^{(21)}_{\rm osc}$,

$$\sin^2\Phi_{21} = \frac{1}{2}\Big(1 - \cos\left[2\pi L/L^{(21)}_{\rm osc}\right]\Big),$$
$$L^{(21)}_{\rm osc} \equiv \frac{4\pi E}{\Delta m^2_{21}}, \qquad L^{(21)}_{\rm osc}[m] \simeq 2.48\ \frac{E[\mathrm{MeV}]}{\Delta m^2_{21}[\mathrm{eV}^2]}, \tag{3.4c}$$

which is the length for obtaining a half-cycle of oscillation. If conditions are such that $2\pi L \ll L^{(21)}_{\rm osc}$, oscillations will not have had a chance to occur because the oscillation phase is too small. Finally, we stress that Eq. (3.4a) is a result of the two-flavor restriction. Although 'three-flavor' phenomenology was already advocated shortly after the discovery of the τ lepton [DeLMPP 80] and is currently used in precise analyses of neutrino data, e.g., [FoTV 12], it can happen that the two-flavor approach is a valid approximation in certain circumstances (see Prob. 2 at the end of this chapter). For example, it is often used to describe both solar mixing ($\theta_{12} \to \theta_\odot$, $\Delta m^2_{21} \to \Delta m^2_\odot$) and atmospheric mixing ($\theta_{23} \to \theta_{\rm A}$, $|\Delta m^2_{32}| \to |\Delta m^2_{\rm A}|$).

We have been considering the vacuum propagation of neutrinos. The *vacuum evolution equation* for the relativistic energy eigenstates ν_1 and ν_2 as expressed in the energy basis is $i d\nu_E/dx = \mathbf{H}_E \nu_E$, where

$$\nu_E \equiv \begin{pmatrix}\nu_1\\ \nu_2\end{pmatrix} \qquad \text{and} \qquad \mathbf{H}_E = \begin{pmatrix}E_1 & 0\\ 0 & E_2\end{pmatrix} \ \to\ \begin{pmatrix}\frac{m_1^2}{2E} & 0\\ 0 & \frac{m_2^2}{2E}\end{pmatrix}. \tag{3.5}$$

[6] As will be discussed in Sect. VI–4, the predicted oscillation pattern of Eq. (3.4a) was first observed in 2002 (for electron antineutrinos) by the KamLAND collaboration.

https://doi.org/10.1017/9781009291033.007 Published online by Cambridge University Press

The right-most matrix form in Eq. (3.5) has been obtained by expanding the energy in powers of the momentum, followed by the phase transformation $\nu_E \rightarrow \exp(-ipx)\nu_E$. Proceeding to the weak basis ν_W,

$$\nu_W \equiv \begin{pmatrix} \nu_e \\ \nu_\mu \end{pmatrix} = \mathbf{U}\nu_E \qquad \text{and} \qquad \mathbf{U} = \begin{pmatrix} \cos\theta_{12} & \sin\theta_{12} \\ -\sin\theta_{12} & \cos\theta_{12} \end{pmatrix}, \tag{3.6a}$$

the evolution equation can be written $id\nu_W/dx = \mathbf{H}_W\nu_W$, where

$$\mathbf{H}_W = \mathbf{U}\mathbf{H}_E\mathbf{U}^{-1} = \begin{pmatrix} -\frac{\Delta m^2_{21}}{4E}\cos 2\theta_{12} & \frac{\Delta m^2_{21}}{4E}\sin 2\theta_{12} \\ \frac{\Delta m^2_{21}}{4E}\sin 2\theta_{12} & \frac{\Delta m^2_{21}}{4E}\cos 2\theta_{12} \end{pmatrix}. \tag{3.6b}$$

As shown earlier in this section, the evolution in Eq. (3.6b) describes $\nu_e \leftrightarrow \nu_\mu$ vacuum oscillations. Using the current PDG value for θ_{12} (see Eq. (II–4.24)), we have from Eq. (3.6a) the numerical expressions

$$|\nu_1\rangle = 0.83|\nu_e\rangle - 0.56|\nu_\mu\rangle, \qquad |\nu_2\rangle = 0.56|\nu_e\rangle + 0.83|\nu_\mu\rangle. \tag{3.6c}$$

The dominant component of $|\nu_2\rangle$ resides in $|\nu_\mu\rangle$, a fact we will refer to in the next section.

Oscillations in matter: MSW effect

Neutrino propagation in matter is a problem of intrinsic theoretical interest. It is also of practical importance because many past and present experiments involve, in part, neutrinos traveling in the interiors of the Sun and of the Earth. In the following, we consider a neutrino moving radially with position coordinate r and continue to employ the two-flavor description.

For neutrino propagation in *matter*, a key difference with the vacuum description is that the neutrinos will undergo $W^\pm$ and Z^0 exchange scattering from atomic electrons and quarks confined within protons and neutrons. Only elastic scattering in the forward direction maintains the coherence of the initial mixed ν_e–ν_μ state. In particular, the quark contributions cancel and it is $W^\pm$ exchange in the ν_e–e interaction which produces a potential difference between electron and muon neutrinos,

$$\Delta V \equiv V(\nu_e) - V(\nu_\mu) = \sqrt{2}G_F N_e(r), \tag{3.7}$$

where $N_e(r)$ is the electron number density at distance r from the origin. That neutrinos in matter experience this potential energy was first pointed out by Wolfenstein [Wo 78], who cited a well-known analogous effect in K^0–$\bar{K}^0$ mixing as neutral kaons move through nuclear matter. To properly account for the Wolfenstein effect, we must alter the diagonal matrix elements in Eq. (3.6b) to

https://doi.org/10.1017/9781009291033.007 Published online by Cambridge University Press

$$\mathbf{H}^{(\mathrm{M})}(r) \equiv \begin{pmatrix} \sqrt{\frac{1}{2}} G_F N_e(r) - \dfrac{\Delta m^2_{21}}{4E} \cos 2\theta_{12} & \dfrac{\Delta m^2_{12}}{4E} \sin 2\theta_{12} \\ \dfrac{\Delta m^2_{12}}{4E} \sin 2\theta_{12} & -\sqrt{\frac{1}{2}} G_F N_e(r) + \dfrac{\Delta m^2_{21}}{4E} \cos 2\theta_{12} \end{pmatrix}, \tag{3.8}$$

where the superscript in $\mathbf{H}^{(\mathrm{M})}$ refers to 'matter'. Since the electron number density is generally spatially dependent, the above matrix $\mathbf{H}^{(\mathrm{M})}$ will have spatially dependent eigenvalues $E_{\pm}(r)$,

$$E_{\pm}(r) = \pm \frac{1}{4} \left[\left(4\mathbf{H}^{(\mathrm{M})}_{\mathbf{11}}(r) \right)^2 + \left(\frac{\Delta m^2_{21}}{E} \sin 2\theta_{12} \right)^2 \right]^{1/2}. \tag{3.9}$$

In the discussion to follow, we shall consider neutrino propagation in the Sun. At the solar core $r = 0$, the potential energy of Eq. (3.7) becomes $\Delta V^{(\mathrm{core})} \simeq 7.6 \times 10^{-12}$ eV upon taking $\sqrt{2} G_F \simeq 7.63 \times 10^{-14}$eV-cm$^3/N_A$ and $N_e^{(\mathrm{core})} \simeq 100 N_A$ cm$^{-3} \simeq 6.0 \times 10^{25}$ cm^{-3}. Let us next make two working hypotheses:

(1) We assume that the electron number density $N_e^{(\mathrm{core})}$ is sufficiently large to ensure that $\mathbf{H}^{(\mathrm{M})}_{\mathbf{11}}(0) > 0$ at the core. Using the value of $N_e^{(\mathrm{core})}$ just given above and adopting the current PDG values for Δm^2_{21} and θ_{12}, this will be valid for neutrinos with energy above $E \sim 2$ MeV. This energy is, however, not precisely fixed since the core is a region and not just a point.

If indeed $\mathbf{H}^{(\mathrm{M})}_{\mathbf{11}}$ is positive at the solar core, it becomes negative before reaching the surface (since N_e vanishes at the surface) and vice versa for $\mathbf{H}^{(\mathrm{M})}_{\mathbf{22}}$. The matrix elements $\mathbf{H}^{(\mathrm{M})}_{\mathbf{11}}$ and $\mathbf{H}^{(\mathrm{M})}_{\mathbf{22}}$ thus cross at the point where each vanishes. In the limit of neglecting the off-diagonals of $\mathbf{H}^{(\mathrm{M})}$, the diagonals become the eigenvalues and we have the phenomenon of *level crossing*, familiar from atomic and nuclear physics. In reality, the off-diagonals do not vanish and so the level crossing is avoided.

(2) We assume that propagation of an electron neutrino in the solar matter is *adiabatic*, i.e. the fractional change in the electron density of the matter is small per neutrino oscillation cycle. If so, a neutrino that starts in one of the energy eigenstates will not experience a transition as it passes through the solar medium. This is akin to a particle in an eigenstate of the one-dimensional infinite well maintaining its quantum state as the wall separation changes sufficiently slowly.

Let us now follow the behavior of $E_{\pm}(r)$ from the solar core at $r = 0$ to the solar surface at $r = R_{\odot}$. As we move outward from the core, $N_e(r)$ will decrease[7] until a point $r = r_{\mathrm{res}}$ is reached at which $\mathbf{H}^{(\mathrm{M})}_{\mathbf{11}}(r_{\mathrm{res}}) = \mathbf{H}^{(\mathrm{M})}_{\mathbf{22}}(r_{\mathrm{res}}) = 0$, with

[7] A popular model for the number density profile is $N_e(r) = N_e(0) e^{-r/r_0}$ with $r_0 \simeq R_{\odot}/10$.

https://doi.org/10.1017/9781009291033.007 Published online by Cambridge University Press

Table VI–1. *Evolution of* $|\nu_2^{\rm M}(r)\rangle$.

r	$\theta(r)$	$\lvert\nu_2^{\rm M}(r)\rangle$
0	$\pi/2$	$\lvert\nu_e\rangle$
$r_{\rm res}$	$\pi/4$	$\left(\lvert\nu_e\rangle + \lvert\nu_\mu\rangle\right)/\sqrt{2}$
$R_\odot$	θ_{12}	$\sin\theta_{12}\lvert\nu_e\rangle + \cos\theta_{12}\lvert\nu_\mu\rangle$

$$N_e^{(\rm res)} \equiv \frac{\Delta m_{12}^2 \cos 2\theta_{12}}{2\sqrt{2} G_F E}, \tag{3.10}$$

after which $E_+(r)$ grows until the surface is reached. Similarly, E_- will increase from $r = 0$ to $r = r_{\rm res}$ and decrease thereafter. The label *res* used here stands for 'resonance', as will be explained shortly.

The eigenstates $|\nu^{\rm M}(r)\rangle$ of the matrix $\mathbf{H}^{(\rm M)}$ are likewise spatially dependent,

$$\begin{aligned} |\nu_1^{\rm M}(r)\rangle &= \cos\theta(r)|\nu_e\rangle + \sin\theta(r)|\nu_\mu\rangle, \\ |\nu_2^{\rm M}(r)\rangle &= -\sin\theta(r)|\nu_e\rangle + \cos\theta(r)|\nu_\mu\rangle, \end{aligned} \tag{3.11}$$

as is also the associated mixing angle $\theta(r)$ which, after some algebra, can be written as

$$\sin 2\theta(r) = \frac{\sin 2\theta_{12}}{\left[\left(N_e(r)/N_e^{(\rm res)} - 1\right)^2 \cos^2 2\theta_{12} + \sin^2 2\theta_{12}\right]^{1/2}}. \tag{3.12}$$

The square of this relation has the profile of a Lorentzian distribution, indicating the presence of a resonance [MiS 85].

Suppose an electron neutrino ν_e is created at the solar core $r = 0$ under the assumption $N_e(0) \gg N_e^{(\rm res)}$. Its evolution to the solar surface $r = R_\odot$ is briefly summarized in Table VI–1 and explained as follows. The condition $N_e(0) \gg N_e^{(\rm res)}$ implies from Eq. (3.12) that $\theta(0) \simeq \pi/2$, and so from Eq. (3.11) that $|\nu_2^{\rm M}\rangle \simeq |\nu_e\rangle$ at the core. Thus, a newly created electron neutrino will reside in the energy eigenstate $|\nu_2^{\rm M}\rangle$ as it begins its journey to the solar surface. If the matter eigenstates undergo adiabatic flow through the resonance, then $|\nu_2^{\rm M}\rangle$ suffers no transitions. As the surface is eventually approached, the electron number density decreases to zero, $N_e(R_\odot) = 0$ and so, from Eq. (3.12), $\theta(r) \to \theta(R_\odot) \simeq \theta_{12}$, the vacuum mixing angle. What is new and exciting is that electron neutrinos of sufficiently high energies, which are created by nuclear reactions at the solar core, have an appreciable probability for conversion to muon neutrinos by the time the solar surface is reached. This is, in essence, the phenomenon known as the Mikheyev–Smirnov–Wolfenstein (MSW) effect [Wo 78, MiS 85]. The mixing between electron and muon type neutrinos has occurred within the Sun and since $|\nu_2\rangle$ is an energy

https://doi.org/10.1017/9781009291033.007 Published online by Cambridge University Press

eigenstate, no further mixing occurs en route to Earth. Measurement at a detector on Earth will yield either ν_e or ν_μ according to the quantum state $|\nu_2\rangle$ of Eq. (3.6c).

Not all neutrinos created in the solar core will experience MSW mixing. As shown earlier, it may be that the neutrino energy is too small (roughly $E_{\nu_e} < 2$ MeV) for level crossing to take place. Or the neutrino flow to the solar surface may not be adiabatic. The quantitative condition for adiabaticity is most stringent at the resonant point $r = r_{\rm res}$,

$$\frac{\sin^2 2\theta_{12}}{\cos 2\theta_{12}} \frac{\Delta m^2_{21}}{2E} \left| \frac{N_e^{(\rm res)}}{N_e'(r_{\rm res})} \right| \gg 1, \tag{3.13}$$

where $N_e'(r_{\rm res})$ is the density gradient, $N_e' \equiv dN_e/dr$, evaluated at the resonant point. Thus, adiabaticity will occur provided the solar electron number density does not change too rapidly with position. The relation in Eq. (3.13) amounts to demanding that the splitting between the energy eigenvalues $E_\pm(r)$ of $\mathbf{H}^{(\rm M)}$ (cf. Eq. (3.9)), which is minimal at the resonant point, nonetheless be much larger than the off-diagonal matrix elements of $\mathbf{H}^{(\rm M)}$ (which would produce transitions between the energy eigenstates). We return to this subject in Sect. VI–4, where we further discuss solar neutrinos.

CP violation

The *CP*-violating phase in the PMNS matrix has physical implications in neutrino oscillations, relating the oscillations of neutrinos to those of antineutrinos. It is reasonably straightforward to use the general form of the oscillation formula to calculate the difference of the oscillation probabilities,

$$A_{ij} \equiv P_{\nu_i \to \nu_j} - P_{\bar\nu_i \to \bar\nu_j} = 4 \sum_{k>\ell} {\rm Im}(U_{ik} U^*_{jk} U_{jl} U^*_{il}) \sin\left(\frac{\Delta m^2_{kl} L}{2E} \right). \tag{3.14}$$

It is less straightforward to measure this. We note that A_{ij} vanishes unless all three flavors of neutrinos are involved. This can be found from direct calculation but is easy to understand on general principles, as the *CP*-violating phase can be removed from any 2×2 submatrix by redefining the fields. Moreover, the numerator in this asymmetry is the same for any $i \neq j$,

$$\begin{aligned} A_{ij} = {} & \sin\delta \cos\theta_{13} \sin 2\theta_{13} \sin 2\theta_{23} \sin 2\theta_{12} \\ & \times \left[\sin\left(\frac{\Delta m^2_{21} L}{2E} \right) + \sin\left(\frac{\Delta m^2_{13} L}{2E} \right) + \sin\left(\frac{\Delta m^2_{32} L}{2E} \right) \right], \end{aligned} \tag{3.15}$$

where we have used $\Delta m^2_{13} = -\Delta m^2_{31}$. We see that two independent mass differences, e.g., Δm^2_{21} and Δm^2_{13}, contribute. In addition, the asymmetry will produce small corrections to the oscillations with the largest amplitudes and will

https://doi.org/10.1017/9781009291033.007 Published online by Cambridge University Press

be most visible for oscillations where the *CP*-even transitions are the smallest, such as $\nu_e \leftrightarrow \nu_\mu$. Although uncovering *CP* violation in oscillations will be an experimental challenge, the rewards of such a measurement will be considerable. For example, lepton *CP* violation is a necessary ingredient for leptogenesis (cf. Sect. VI–6).

VI–4 Neutrino phenomenology

Determination of the set of mixing parameters $\{\theta_{ij}\}$ and $\{\Delta m^2_{ij}\}$ has taken years of careful experimentation. This has involved a variety of neutrino sources, including our Sun, the Earth's atmosphere, nuclear reactors and particle accelerators. Many references and detailed accounts exist in the literature.[8]

Solar and reactor neutrinos: θ_{12} and Δm^2_{21}

Solar neutrinos: The current evaluations [RPP 12] of the parameters $\sin^2 2\theta_{12}$ and Δm^2_{21} from a three-neutrino fit give

$$\sin^2 2\theta_{12} = 0.857 \pm 0.024 \qquad \Delta m^2_{21} = (7.50 \pm 0.20) \times 10^{-5}\ \mathrm{eV}^2. \qquad (4.1)$$

This represents an uncertainty of under 3%, which is one indication of how successful the search for these basic parameters has turned out. The earliest progress in this area involved the detection of solar neutrinos. It was Davis [Da 64] who used a chlorine detector to probe solar neutrinos and Bahcall [Ba 64] who provided the theoretical basis for such an ambitious undertaking. An important conceptual contribution came from Pontecorvo, who suggested testing whether leptonic charge was conserved, and who wrote 'From the point of view of detection possibilities, an ideal object is the Sun' [Po 68].

The initial intent of the chlorine experiment was actually to test physics at the core of the Sun. A significant achievement of solar neutrino studies has been to demonstrate that stars are, indeed, powered by nuclear fusion reactions. Energy produced by the Sun arises from thermonuclear reactions in the solar core and the underlying theoretical description is called the Standard Solar Model (SSM). Solar burning utilizes all three types of Standard Model reactions – strong, weak, and electromagnetic – as well as using gravity to provide the required high density. The primary ingredients of the SSM are:

(1) The Sun evolves in hydrostatic equilibrium, balancing the gravitational force and the pressure gradient. The equation of state is specified as a function of temperature, density, and solar composition.

[8] Some recent examples include [AnMPS 12], [Ba 90], [BaH 13], [FoTV 12], [FoLMMPR 12], [GiK 07], [GoMSS 12], [HaRS 12], [KiL 13], [MoA *et al.* 07], and Chap. XIII in [RPP 12] by Nakamura and Petkov.

https://doi.org/10.1017/9781009291033.007 Published online by Cambridge University Press

(2) Energy proceeds through the solar medium by radiation and convection. While the solar envelope is convective, radiative transport dominates the core region where the thermonuclear reactions take place.
(3) The primary thermonuclear chain involves the conversion $4p \rightarrow {}^4\mathrm{He} + 2e^+ + 2\nu_e$. This *pp* chain produces 26.7 MeV per cycle, and the associated neutrino production rate is firmly tied to the amount of energy production. The core temperature and electron number density of the Sun are respectively $T_c \sim 1.5 \times 10^7$ K and $N_e \sim 6 \times 10^{25}\,\mathrm{cm}^{-3}$.
(4) The model is constrained to produce the observed solar radius, mass and luminosity. The initial ^{4}He/H ratio is adjusted to reproduce the luminosity at the Sun's current 4.57 Giga-year age.

The dominant process is the '*pp* chain', occurring in stages I → IV:

Stage		Nuclear reaction	Br (%)
I		$p + p \rightarrow {}^2\mathrm{H} + e^+ + \nu_e$	99.75
		$p + e + p \rightarrow {}^2\mathrm{H} + \nu_e$	0.25
II		${}^2\mathrm{H} + p \rightarrow {}^3\mathrm{He} + \gamma$	100.00
III		${}^3\mathrm{He} + {}^3\mathrm{He} \rightarrow {}^4\mathrm{He} + 2p$	86.00
	or	${}^3\mathrm{He} + {}^4\mathrm{He} \rightarrow {}^7\mathrm{Be} + \gamma$	14.00
IV		${}^7\mathrm{Be} + e^- \rightarrow {}^7\mathrm{Li} + \nu_e$	99.89
		${}^7\mathrm{Li} + p \rightarrow {}^4\mathrm{He} + {}^4\mathrm{He}$	
	or	${}^7\mathrm{Be} + p \rightarrow {}^8\mathrm{B} + \gamma$	0.11
		${}^8\mathrm{B} \rightarrow {}^8\mathrm{Be}^* + e^+ + \nu_e$	

Let us isolate those processes which produce neutrinos and order them according to increasing maximum neutrino energy:

Label	Reaction	$E^{\nu}_{\max}$(MeV)
pp	$p + p \rightarrow {}^2\mathrm{H} + e^+ + \nu_e$	0.42
^{7}Be	${}^7\mathrm{Be} + e^- \rightarrow {}^7\mathrm{Li} + \nu_e$	0.86
pep	$p + e + p \rightarrow {}^2\mathrm{H} + \nu_e$	1.44
^{8}B	${}^8\mathrm{B} \rightarrow {}^8\mathrm{Be}^* + e^+ + \nu_e$	14.06
hep	${}^3\mathrm{He} + p \rightarrow {}^4\mathrm{H} + e^+ + \nu_e$	18.47

The energy spectra of the *pp*, ^{8}B and *hep* neutrinos are continuous whereas the *pep* and ^{7}Be neutrinos are monoenergetic. Within this general framework, there is, however, still a degree of theoretical uncertainty and work continues to this day on solar modeling. Table VI–2 (taken from [HaRS 12] and [AnMPS 12]) lists SSN flux predictions according to two sets, labelled GS98 and AGSS09, and taken respectively from [GrS 98] and [AsBFS 09]. Note the marked decrease in flux with increasing neutrino energy.

https://doi.org/10.1017/9781009291033.007 Published online by Cambridge University Press

Table VI–2. *Neutrino flux*[a] *in the pp chain.*

Label	GS98	AGSS09	Solar data
pp	$5.98(1 \pm 0.006) \times 10^{-1}$	$6.03(1 \pm 0.006) \times 10^{-1}$	$6.05(1^{+0.003}_{-0.011})$
^{7}Be	$5.00(1 \pm 0.07) \times 10^{-1}$	$4.561(1 \pm 0.07) \times 10^{-1}$	$4.82(1^{+0.05}_{-0.04}) \times 10^{-1}$
pep	$1.44(1 \pm 0.012) \times 10^{-1}$	$1.47(1 \pm 0.012) \times 10^{-1}$	$1.46(1^{+0.010}_{-0.014}) \times 10^{-2}$
^{8}B	$5.58(1 \pm 0.13) \times 10^{-1}$	$4.59(1 \pm 0.13) \times 10^{-1}$	$5.25(1 \pm 0.038) \times 10^{-4}$
hep	$8.04(1 \pm 0.30) \times 10^{-1}$	$8.31(1 \pm 0.30) \times 10^{-1}$	—

[a]Expressed in units of $10^{10}\text{cm}^{-2}\text{s}^{-1}$.

On the basis of such flux predictions, results from various solar neutrino experiments could be compared with the SSM. The following compilation, taken from [AnMPS 12], summarizes early results for the ratio of observed-to-predicted electron neutrino flux,

Homestake	0.34 ± 0.03,	Super-K	0.46 ± 0.02,
SAGE	0.59 ± 0.06,	Gallex,GNO	0.58 ± 0.05.

We now know that this spread of values arises from the interplay between the range of neutrino energies and the influence of the MSW effect. At the time, however, it was unclear whether the SSM itself was at fault. The issue was resolved by a series of experiments which probed flavor mixing of solar neutrinos while simultaneously testing the SSN prediction for the total solar flux. This was carried out by the SNO collaboration; for a summary see [Ah *et al.* (SNO collab.) 11]. Since the SNO detector employed heavy water, there was sensitivity to the three reactions:

$$\begin{aligned}
&\text{charged current (CC):} && \nu_e + d \to p + p + e^- && \\
&\text{neutral current (NC):} && \nu_x + d \to p + n + \nu_x && (x = e, \mu, \tau) \\
&\text{elastic scattering (ES):} && \nu_x + e^- \to \nu_x + e^- && (x = e, \mu, \tau).
\end{aligned} \tag{4.2}$$

In the Standard Model, only ν_e contributes to the CC reaction, but all neutrino flavors contribute, with equal rates, to the the NC reactions (and also to the ES, but with ν_e having about six times the rate of ν_μ and ν_τ). Early CC measurements found $f_{\nu_e}^{(\text{CC})} = (1.76 \pm 0.11) \times 10^6\ \text{cm}^{-2}\,\text{s}^{-1}$, much less than the (then) predicted total flux $f_{\nu_e}^{\text{tot}} = (5.05 \pm 0.91) \times 10^6\ \text{cm}^{-2}\,\text{s}^{-1}$. Then, NC measurements obtained $f_{\nu_e}^{(\text{NC})} = (5.09 \pm 0.62) \times 10^6\ \text{cm}^{-2}\,\text{s}^{-1}$, consistent with the $f_{\nu_e}^{\text{tot}}$ prediction. Within errors, the only reasonable explanation is that the conversion of $\nu_e \to \nu_\mu, \nu_\tau$ must be occurring. A more recent determination of the total flux from the ^{8}B reaction reduces the uncertainty,

$$\Phi_{^8\text{B}}^{(\text{tot})} = \left(5.25 \pm 0.16\ (\text{stat})\ {}^{+0.11}_{-0.13}\ (\text{syst})\right) \times 10^6\ \text{cm}^{-2}\,\text{s}^{-1}, \tag{4.3}$$

https://doi.org/10.1017/9781009291033.007 Published online by Cambridge University Press

consistent with but having smaller uncertainty than the SSN predictions of Table VI–2.

In summary, the versatility of solar neutrino experiments is that they are sensitive to various nuclear reactions in the Sun through the measurement of different energy neutrinos. The survival probability for electron neutrinos to reach the Earth will depend on the neutrino energy E and will in part be affected by the solar MSW effect. The survival probability in the two-flavor description can be expressed as [Pa 86]

$$\overline{\mathcal{P}}_{\nu_e \to \nu_e} = \frac{1}{2} + \left(\frac{1}{2} - \mathcal{P}_{\text{non-adbtc}} \right) \cos 2\theta(0) \cos 2\theta_{12}. \tag{4.4a}$$

In the above, $\theta(0)$ represents the matter mixing angle at the point of neutrino production (taken here at $r = 0$), averaging of oscillatory behavior has been carried out, and $\mathcal{P}_{\text{non-adbtc}}$ describes the nonadiabatic mixing (which is sensitive to the electron number density $N_e(r)$) as in Eq. (3.13).

Let us explore Eq. (4.4a) in the limits of low-energy and high-energy neutrino energy, while assuming just adiabatic transitions ($\mathcal{P}_{\text{non-adbtc}} = 0$). For very low-energy neutrinos, as explained previously, there is no MSW resonance and the the situation reduces to simple vacuum mixing,

$$\overline{\mathcal{P}}_{\nu_e \to \nu_e} = 1 - \frac{1}{2} \sin^2 2\theta_{12} \simeq 0.57, \tag{4.4b}$$

whereas for very energetic neutrinos, we have $\theta(0) \simeq \pi/2$ and so

$$\overline{\mathcal{P}}_{\nu_e \to \nu_e} = \sin^2 2\theta_{12} \simeq 0.31. \tag{4.4c}$$

For intermediate neutrino energy, the average survival probability interpolates smoothly between these two limits. The overall pattern is as depicted in Fig. VI–1. The recent experiment [Be *et al*. (Borexino collab.) 12a] on *pep* neutrinos, whose energy $E = 1.44$ MeV is at the low end of the spectrum, finds a survival probability $\overline{\mathcal{P}}_{\nu_e \to \nu_e} = 0.62 \pm 0.17$, which is in accord with the above analysis.

The relations in Eqs. (4.4a–c) pertain to neutrino propagation directly from the Sun to the Earth. This is referred to as 'daytime' detection, sometimes denoted by $\overline{\mathcal{P}}^{(\text{D})}_{\nu_e \to \nu_e}$. The 'nighttime' probability $\overline{\mathcal{P}}^{(\text{N})}_{\nu_e \to \nu_e}$ would be sensitive to matter effects from passage through the Earth. Letting R_{D} and R_{N} represent the day and night counting rates, the 'day–night' asymmetry,

$$\mathcal{A}_{\text{D–N}} \equiv 2 \frac{R_{\text{N}} - R_{\text{D}}}{R_{\text{N}} + R_{\text{D}}}, \tag{4.5}$$

https://doi.org/10.1017/9781009291033.007 Published online by Cambridge University Press

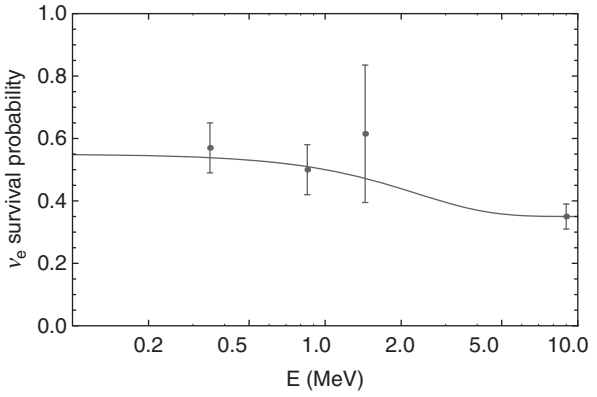

Fig. VI–1 Average survival probability of solar neutrinos vs. neutrino energy. Data points represent (from left to right) *pp*, ^{7}Be, *pep*, and ^{8}B neutrinos.

is an observable which isolates the effect of Earth matter on neutrino propagation. This is in distinction to the MSW effect in the Sun, which cannot be turned off. Several experiments, the SNO and Super-K experiments (with ^{8}B) and Borexino (with ^{7}Be) have studied the day–night effect. For example, the results [Be *et al.* (Borexino collab.) 12b],

$$\begin{aligned} \mathcal{A}_{\mathrm{D-N}} &= -\,(0.1 \pm 1.2 \pm 0.7)\,\% \qquad \text{[Borexino]} \\ &= -\,(4.0 \pm 1.3 \pm 0.8)\,\% \qquad \text{[Super-K]}, \end{aligned} \tag{4.6}$$

are consistent with the theory predictions $|\mathcal{A}_{\mathrm{D-N}}| \leq 0.1\%$ (Borexino) and $\mathcal{A}_{\mathrm{D-N}} \simeq -3\%$ (Super-K), although the latter is also 2.6σ from zero.

Reactor antineutrinos: The KamLAND experiment was able to observe oscillations of $\bar{\nu}_e$ antineutrinos under laboratory conditions. The $\bar{\nu}_e$ beam originates from nuclear beta decays from several nuclear reactors and detection is obtained via the inverse beta-decay process

$$\bar{\nu}_e + p \to e^+ + n. \tag{4.7}$$

In the KamLAND experiment, the average baseline between sources and detector is $L_0 \sim 180$ km and the antineutrino energy spectrum covers the approximate range $1 \leq E_{\bar{\nu}_e} \leq 7$ MeV. The $\bar{\nu}_e$ survival formula, as in Eq. (3.4), suggests plotting the data as a function of $L_0/E_{\bar{\nu}_e}$. The result, shown in Fig. VI–2, clearly exhibits the oscillation pattern. This important observation yielded the most accurate determination of Δm^2_{21} at the time and continues to be a significant contributor to the current database.[9]

[9] Since properties of electron antineutrinos are being studied, it is necessary to assume the validity of *CPT* invariance to compare the KamLAND results with those from solar neutrino studies (and any other experiment using neutrinos and not antineutrinos).

https://doi.org/10.1017/9781009291033.007 Published online by Cambridge University Press

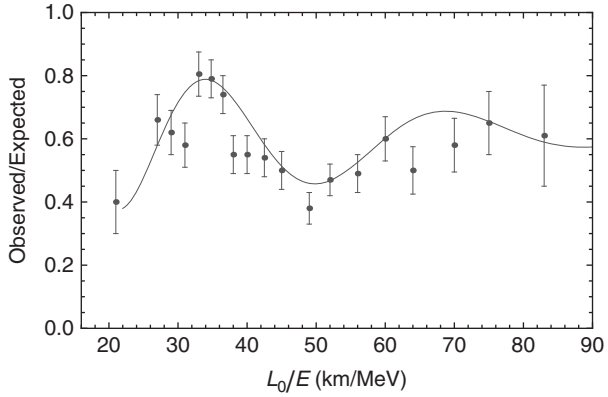

Fig. VI–2 Authors' representation of the KamLAND observation of neutrino oscillations. The curve represents a fit to the oscillation hypothesis.

Atmospheric and accelerator neutrinos: θ_{23} and $|\Delta m^2_{32}|$

Since 1996, the Super-Kamiokande experiment has utilized a 50-kiloton Cherenkov detector to study oscillations of so-called 'atmospheric' muon neutrinos. When high-energy cosmic rays strike the Earth's atmosphere a multitude of secondary particles are produced, most of which travel at nearly the speed of light in the same direction as the incident cosmic ray. Many of the secondaries are pions and kaons, which decay into electrons, muons, and their neutrinos. Using known cross sections and decay rates, one expects about twice as many muon neutrinos as electron neutrinos from the cosmic-ray events. For example, a π^+ decays predominantly as

$$\pi^+ \to \mu^+ + \nu_\mu \to e^+ + \nu_e + \bar{\nu}_\mu + \nu_\mu,$$

i.e., two muon-type neutrinos are produced but only one that is electron-type. Detection of these atmospheric neutrinos yielded evidence for oscillations, to wit, a deficit of muon-type neutrinos, but *no* such deficit for the electron neutrinos. This has since been augmented with data containing dependence on the azimuthal angle (and hence distance from the source) and on the neutrino energy. Because the deficit is of just muon neutrinos, the hypothesis is that these oscillations involve the conversion $\nu_\mu \to \nu_\tau$. Any ν_τ thus generated is not energetic enough to react via the charged current to produce a τ.

Accelerator-based efforts to probe the same oscillation parameters include the K2K and MINOS experiments. In particular, since 2005 MINOS has studied muon neutrinos originating from Fermilab and traveling 735 km through the Earth to a detector at the Soudan mine in the state of Minnesota. At Fermilab, an injector beam of protons strikes a target, producing copious numbers of pions, whose decay is the source of muon neutrinos.

https://doi.org/10.1017/9781009291033.007 Published online by Cambridge University Press

Data from both the Super-Kamiokande and MINOS experiments support the $\nu_\mu \to \nu_\tau$ scenario with mixing angle and mass difference given by [RPP 12]:

$$\sin^2 2\theta_{23} > 0.95 \qquad |\Delta m^2_{32}| = 0.00232^{+0.0012}_{-00008}\ \text{eV}^2. \tag{4.8}$$

Moreover, each experiment has also studied muon *anti*neutrino oscillations, finding mixing parameters consistent with these values, although less precisely determined.

Finally, the T2K collaboration announcement in 2012 of the first evidence for ν_e appearance in a ν_μ beam has been confirmed in a recent update [Ab *et al*. (T2K collab.) 13]. The ν_e appearance probability at oscillation maximum is

$$\mathcal{P}_{\nu_\mu \to \nu_e} \simeq 4c^2_{13}s^2_{13}s^2_{23}\left[1 + \frac{2a}{\Delta m^2_{31}}\right] - 8c^2_{13}c_{12}c_{23}s_{12}s_{13}s_{23}\Phi_{21}\sin\delta, \tag{4.9}$$

where $\Phi_{21} \equiv \Delta m^2_{21}L/(4E)$ and $a \equiv 2\sqrt{2}G_F n_e E$. In particular, the value of $\sin^2(2\theta_{13})$ inferred from the data depends on whether a normal or inverted neutrino mass hierarchy is assumed. This can, in turn, be compared to reactor values for $\sin^2(2\theta_{13})$. Thus, the importance of this type of experiment lies in its sensitivity both to the hierarchy issue and to detection of a *CP*-violating signal ($\delta \neq 0$). Future data from the T2K and NOνA experiments have the potential for significant progress in our understanding of neutrino physics.

Short-baseline studies: θ_{13}

The last of the neutrino oscillation angles to be determined with precision is θ_{13}. Initial fits to mixing data indicated their smallness. This led to the concern that signals of neutrino *CP* violation, i.e., determination of the *CP*-violating phase δ, might be experimentally inaccessible. For example, recall from Eq. (3.15) that the *CP*-violating asymmetry A_{ij} is linear in both $\sin\delta$ and $\sin\theta_{13}$. Hence, the attempt to measure θ_{13} took on a certain urgency.

Following a growing number of indications that indeed $\theta_{13} \neq 0$, it was several reactor short-baseline experiments which provided the needed precision. A key point is that in $\bar{\nu}_e$ disappearance experiments, with a relatively short baseline of roughly 1 km, the influence of $\sin^2(2\theta_{12})$ and Δm^2_{21} on the survival probability $\mathcal{P}^{(\text{surv})}_{\bar{\nu}_e}$ for electron antineutrinos can safely be neglected. We then have (see Prob. VI–2),

$$\begin{aligned}\mathcal{P}^{(\text{surv})}_{\bar{\nu}_e} &\simeq 1 - 2|U_{13}|^2\left(1 - |U_{13}|^2\right)\left(1 - \cos\left[\frac{\Delta m^2_{31}}{2E}L\right]\right)\\ &= 1 - \sin^2(2\theta_{13})\sin^2\left(1.267\Delta m^2_{31}L/E\right).\end{aligned} \tag{4.10}$$

https://doi.org/10.1017/9781009291033.007 Published online by Cambridge University Press

Based on data from the collaborations Daya Bay [An *et al*. 12], RENO [Ahn *et al*. 12] and Double Chooz [Abe *et al*. 12], the current RPP listing gives [RPP 12]

$$\sin^2 2\theta_{13} = 0.098 \pm 0.013. \tag{4.11}$$

Finally, the future of short-baseline experiments has the potential for additional interesting findings. In particular, the inverse relation between L and Δm^2 in the neutrino oscillation relations implies that a very short-baseline study (say, with $L \sim 5 \rightarrow 50$ m) would be sensitive to much larger values of squared mass difference (say, having order of magnitude $\Delta m^2 \sim 1$ eV^2) than those observed for Δm^2_{21} and Δm^2_{32}. Such a large neutrino mass difference evidently occurred in the LSND experiment [Ag *et al*. 01 (LSND collab.)], which found evidence at 3.5σ for $\bar{\nu}_\mu \rightarrow \bar{\nu}_e$ oscillations with $\Delta m^2 > 0.2$ eV^2. We shall not discuss this experiment further, except to note that, if validated, it would represent effects (e.g., one or more sterile neutrinos) beyond the Standard Model.

VI–5 Testing for the Majorana nature of neutrinos

In order to determine if the neutrino mass has a Majorana component, one can use the fact that Majorana masses violate lepton-number conservation. A sensitive measure occurs in the process of neutrinoless double beta decay. There are many situations in Nature where one has a nucleus which is kinematically forbidden to decay via ordinary beta decay,

$$^Z A \not\rightarrow {}^{Z-1}A + e^- + \bar{\nu}_e, \tag{5.1}$$

but which is allowed to decay via emission of two lepton pairs ($2\nu\beta\beta$),

$$^Z A \rightarrow {}^{Z-2}A + e^- + e^- + \bar{\nu}_e + \bar{\nu}_e. \tag{5.2}$$

This $2\nu\beta\beta$ process is attributable to the pairing force in nuclei and occurs only for even–even nuclei. It is produced at order G_F^2 through the exchange of two W bosons. When $2\nu\beta\beta$ can occur, it is also kinematically possible to have a *neutrinoless* double beta decay ($0\nu\beta\beta$),

$$^Z A \rightarrow {}^{Z-2}A + e^- + e^-. \tag{5.3}$$

However, this latter process violates lepton-number conservation by two units and would be forbidden if the neutrino possessed a standard Dirac mass. We will see that this becomes a sensitive test of the Majorana nature of neutrino mass.

First, consider $2\nu\beta\beta$ decay. Because this involves five-body phase space as well as two factors of the weak coupling constant G_F this process is very rare, with

https://doi.org/10.1017/9781009291033.007 Published online by Cambridge University Press

Table VI–3. *Half-lives of some two-neutrino double beta emitters.*

Nucleus	$T^{2\nu}_{1/2}$(yr)
^{96}Zr	$(2.0 \pm 0.3 \pm 0.2) \times 10^{19}$
^{76}Ge	$(1.7 \pm 0.2) \times 10^{21}$
^{136}Xe	$(2.23 \pm 0.017 \pm 0.22) \times 10^{21}$
^{76}Ge	$(1.7 \pm 0.2) \times 10^{21}$

lifetimes of order 10^{20} years. Even so, it has been observed in many nuclei, and some examples are cited in Table VI–3. The rate for such processes is

$$\Gamma_{2\nu} \sim m_e^{11} F_2\,(Q/m_e) \left| g_{\rm a}^2 M_{GT} - g_{\rm v}^2 M_F \right|^2 \cdot \frac{\mathcal{F}(Z)}{E_i - \langle E_n \rangle - \frac{1}{2}E_0}, \tag{5.4}$$

where $\mathcal{F}(Z)$ is a Fermi function, $F_2\,(Q/m_e)$ is a kinematic factor,

$$F_2(x) = x^7 \left(1 + \frac{x}{2} + \frac{x^2}{9} + \frac{x^3}{90} + \frac{x^4}{1980}\right), \tag{5.5}$$

and M_F, M_{GT} are, respectively, the Fermi and Gamow–Teller matrix elements,

$$M_F = \langle f | \frac{1}{2} \sum_{ij} \tau_i^+ \tau_j^- | i \rangle, \qquad M_{GT} = \langle f | \frac{1}{2} \sum_{ij} \tau_i^+ \tau_j^- \boldsymbol{\sigma}_i \cdot \boldsymbol{\sigma}_j | i \rangle. \tag{5.6}$$

In Eq. (5.4), the closure approximation has been made to represent a sum over intermediate states via an average excitation energy $\langle E_n \rangle$. The experimental $2\nu\beta\beta$ decay rates then determine these matrix elements, which unfortunately are extremely difficult to determine theoretically.

If the neutrino has a Majorana mass component, then neutrinoless double beta decay is possible. The basic weak process underlying $0\nu\beta\beta$ decay involves the transition $W^-W^- \to e^-e^-$ through the Feynman diagram of Fig. VI–3. Let us initially treat this process by considering only one generation and invoking the mass diagonalization framework of Sect. VI–2. Because the charged weak current couples to

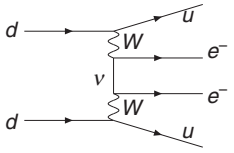

Fig. VI–3 The basic weak process underlying $0\nu\beta\beta$ decay.

https://doi.org/10.1017/9781009291033.007 Published online by Cambridge University Press

the combination (cf. Eqs. (1.3), (1.6)) $\nu_L = \cos\theta\ \nu_b + \sin\theta\ \nu_a^c$, the exchange of the two neutrino eigenstates leads to a matrix element which is proportional to

$$\frac{\sin^2\theta\ m_a}{Q^2 - m_a^2} + \frac{\cos^2\theta\ m_b}{Q^2 - m_b^2}, \tag{5.7}$$

noting that the $\not{q}$ portion of the propagator numerator vanishes due to the chiral relation $\Gamma_L \not{q} \Gamma_L = 0$. If the Majorana mass term is vanishingly small compared to the Dirac mass, this reaction also vanishes since in this case $\theta = \pi/4$ (so that $\sin\theta = \cos\theta$) and $m_a = -m_b = m_D$. Despite the apparent existence of two Majorana fields, the fermion-number violating transition vanishes because the two contributions are equal and opposite.[10]

However, if the Majorana mass term does not vanish, the transition can occur. Let us consider the case of the seesaw mechanism, in which $m_a \simeq m_M \gg M_W$ and $\theta \simeq m_D/m_M \ll 1$. Then the contribution of the first propagator becomes tiny, and a nonvanishing transition occurs due to the second propagator. The process is now directly proportional to the light Majorana mass m_b. The momentum flowing in this propagator is of order the electron mass, so we can neglect the mass dependence m_b^2 in the denominator. This leaves the transition proportional to m_b/Q^2. In this scenario the light neutrino acts like a pure Majorana fermion.

When all three generations of neutrinos can contribute the result depends also on the lepton mixing matrix. If one is dealing with Majorana neutrinos, and neglects the neutrino mass in the denominator of the neutrino propagator, then the figure of merit is the averaged Majorana mass $\langle m_\nu \rangle$ obtained by summing over all neutrino species,

$$\langle m_\nu \rangle \equiv \sum_{i=1}^{3} U_{ie}^2 m_i \ . \tag{5.8}$$

Note that it is the *square* UU of the PMNS matrix, not the usual combination $U^\dagger U$, that enters the reaction. This is because both weak currents lead to e^- emission in the final state. It is this feature which allows the Majorana phases $\alpha_{1,2}$ to contribute to $\langle m_\nu \rangle$. The decay rate for such a neutrinoless decay has a form analogous to that in Eq. (5.4),

$$\Gamma_{0\nu} \sim m_e^7 F_0(Q/m_e) |g_{\rm a} \widetilde{M}_{GT} - g_{\rm v}^2 \widetilde{M}_F|^2 \frac{\langle m_\nu \rangle^2}{m_e^2}, \tag{5.9}$$

[10] If one had chosen to redefine m_b to be positive via a phase redefinition, as described in Sect. VI–1, there would be an extra phase in the weak current of ν_b such that the cancelation would still occur due to a factor of $i^2 = -1$ in the double beta decay matrix element.

https://doi.org/10.1017/9781009291033.007 Published online by Cambridge University Press

except now with the phase space factor $F_0(x)$,

$$F_0(x) = x\left(1 + 2x + \frac{4x^2}{3} + \frac{x^3}{3} + \frac{x^4}{30}\right), \tag{5.10}$$

and nuclear matrix elements

$$\widetilde{M}_F = \langle f|\frac{1}{2}\sum_{ij}\tau_i^+\tau_j^-\frac{1}{r_{ij}}|i\rangle, \qquad \widetilde{M}_{GT} = \langle f|\frac{1}{2}\sum_{ij}\tau_i^+\tau_j^-\sigma_i\cdot\sigma_j\frac{1}{r_{ij}}|i\rangle. \tag{5.11}$$

The factor of $1/r_{ij}$ in Eq. (5.11) comes from spatial dependence associated with the neutrino propagator in the limit that one neglects the neutrino mass in the denominator of Eq. (5.7).

Neutrinoless double beta decay, $0\nu\beta\beta$, is a topic of considerable theoretical importance and is currently under investigation experimentally. As of yet no such mode has been observed. Present limits are $\langle m_\nu\rangle < 140 \to 380$ meV [Ac *et al.* (EXO-200 collab.) 11] and $\langle m_\nu\rangle < 260 \to 540$ meV [Ga *et al.* (KamLAND–ZEN collab.) 12]. There are a number of planned experiments which aim to lower these bounds.

VI–6 Leptogenesis

The material Universe is mostly comprised of matter – protons, neutrons and electrons – rather than their antiparticles. The net baryon asymmetry is described by the ratio

$$\eta_B = \frac{N_B - N_{\bar{B}}}{N_\gamma} \sim 6\times 10^{-10}. \tag{6.1}$$

Because baryon number and other symmetries are violated in the Standard Model and in most of its extensions, it is plausible that this asymmetry was generated dynamically in the early Universe. Such a dynamical mechanism requires a process which is out of thermal equilibrium and which violates both baryon number and *CP* conservation [Sa 67].

If heavy right-handed Majorana neutrinos exist, as allowed by the general mass analysis of the Standard Model, they can generate the net baryon asymmetry. The basic point is that the heavy Majorana particles can decay differently to leptons and antileptons as they fall out of equilibrium in the early Universe through the *CP* violation that is present in the PMNS matrix, and this lepton number asymmetry can be reprocessed into a baryon-number asymmetry through the $B + L$ anomaly of the Standard Model.

The decay of Majorana particles need not conserve lepton number, as the Majorana mass itself violates this quantity. However, to violate *CP* symmetry requires a

https://doi.org/10.1017/9781009291033.007 Published online by Cambridge University Press

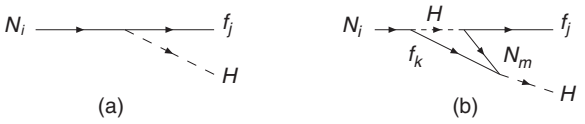

Fig. VI–4 Violating *CP* symmetry in the lepton sector.

specific dynamical mechanism. There can be an interference between the phases of the PMNS matrix and phases generated by unitarity effects for a given final state. To see this, consider the decay diagrams depicted in Fig. VI–4. The tree-level diagrams are proportional to the Yukawa couplings, which are in general complex. However, this is not enough, as an overall phase leads to an unobservable effect when calculating decay rates. But loop diagrams with on-shell intermediate states, like those in Fig. VI–4, pick up extra imaginary parts from on-shell rescattering. Computationally, this comes from the $i\epsilon$ in Feynman propagators. In addition, loop amplitudes have different PMNS phases because they sum over all the particles in the loop. Schematically, this is manifest in decay amplitudes as

$$\begin{aligned} A_{N_i \to H f_j} &= g_{ij} + \sum_{k,m} |L_{km}| e^{i\delta_{km}} g_{ik} g^*_{km} g_{mj}, \\ A_{N_i \to \bar{H} \bar{f}_j} &= g^*_{ij} + \sum_{k,m} |L_{km}| e^{i\delta_{km}} g^*_{ik} g_{km} g^*_{mj}, \end{aligned} \tag{6.2}$$

where the loop diagram is represented by $|L_{km}|e^{i\delta_{km}}$ with a rescattering phase due to on-shell intermediate states δ_{km}. The weak phases in the Yukawa couplings g_{ij} change sign under the change from particle to antiparticle, but the rescattering phase does not. We see that a differential rate develops $|A_{N\to H_j f_i}|^2 - |A_{N\to \bar{H} \bar{f}_i}|^2 \neq 0$ through the interference of tree and loop processes and between the different components of the loop diagram.

Producing a net lepton asymmetry would not be sufficient to explain the observed matter asymmetry unless some of the leptons could be transformed to baryons. This can be accomplished through the baryon anomaly described earlier in Chap. III. In the early Universe, with temperatures above the weak scale, processes which change baryon number, but conserve $B - L$, can occur rapidly. This transfers some of the initial lepton excess into a net number of baryons.

The detailed prediction of the amount of baryon production depends on the size of the *CP*-violating phases, as well as the masses of the heavy Majorana particles. While a unique set of parameters is not available, in general one needs heavy particles of at least 10^9 GeV in order to reproduce the observed asymmetry. This fits well with the observed size of the light neutrino masses, as described earlier in Sect. VI–1.

https://doi.org/10.1017/9781009291033.007 Published online by Cambridge University Press

VI–7 Number of light neutrino species

It might seem that the subject of this section, the number of light neutrino species, is a non-issue. After all, the very structure of the Standard Model has each charged fermion paired with its own neutrino in a weak isospin doublet. Since three charged fermions are known to exist, so there must be three neutrinos. Let us, however, view this purely as an issue of *experimental* physics. In particular, data from Z^0-decay [Sc *et al*. 06] and the cosmic microwave background (CMB) [Hi *et al*. (WMAP collab.) 13] have been used to obtain independent determinations of the number of 'light' neutrino species N_ν. We discuss these two approaches in turn.

Studies at the Z^0 peak

Since final-state neutrinos are the only Standard Model particles *not* detected in Z^0 decay, they contribute to the so-called invisible width $\Gamma_{\rm inv}$. In the Standard Model, this is predicted to be

$$\Gamma_{\rm inv} = \Gamma_Z - \left(\Gamma_{\rm had} + \Gamma_{ee} + \Gamma_{\mu\mu} + \Gamma_{\tau\tau}\right) = (497.4 \pm 2.5)\ \text{MeV}, \tag{7.1}$$

where Γ_Z is the total Z^0 width and $\Gamma_{\rm had}$, Γ_{ee}, $\Gamma_{\mu\mu}$, $\Gamma_{\tau\tau}$ are the hadronic and leptonic widths. But is this what is actually found experimentally?

Several approaches have been explored using the invisible width to determine N_ν, but the one cited here has the advantage of minimizing experimental uncertainties. The trick is to work with the ratio of measured quantities $\Gamma_{\rm inv}/\,\Gamma_{\ell\bar{\ell}}$,

$$\frac{\Gamma_{\rm inv}}{\Gamma_{\ell\bar{\ell}}} = N_\nu \left(\frac{\Gamma_{\nu\bar{\nu}}}{\Gamma_{\ell\bar{\ell}}}\right)_{\rm SM}. \tag{7.2}$$

The interpretation of this relation is clear, that the measured invisible width is the product of the number of light neutrino species N_ν and the decay width into a single neutrino–antineutrino pair. Using data collected from the collection of LEP and SLD experiments,[11] one finds [Sc *et al*. 06]

$$N_\nu = 2.984 \pm 0.008, \tag{7.3}$$

which is consistent with the Standard Model value of $N_\nu = 3$.

Astrophysical data

Astrophysics supplies an independent determination of N_ν which, although currently much less precise, is nonetheless of value. The issue of interest to us is

[11] Certain assumptions are made, among them that lepton universality is valid, and that the top-quark and Higgs masses are respectively $m_t = 178.0$ GeV and $M_H = 150$ GeV. See [Sc *et al*. 06] for additional discussion.

https://doi.org/10.1017/9781009291033.007 Published online by Cambridge University Press

that the CMB has sensitivity, in part, to the neutrino number. Some insight can be gained by considering the thermal content of an expanding Universe. We take the radiation energy density ρ_r as

$$\rho_r = \rho_\gamma + \rho_\nu, \tag{7.4}$$

referring respectively to photons (ρ_γ) and relativistic neutrinos (ρ_ν). The photon and neutrino components obey the well-known thermal relations,

$$\rho_\gamma = \frac{\pi^2}{15} T_\gamma^4, \qquad \rho_\nu = \frac{\pi^2}{15} T_\nu^4 \cdot \frac{7}{8} N_\nu. \tag{7.5}$$

For a temperature somewhat in excess of 10 MeV, the Universe is pervaded by an $e^\pm$, ν, γ plasma in thermal equilibrium via the electroweak interactions (so that $T_\nu = T_\gamma$). As the temperature drops to about 10 MeV, the expansion rate of the Universe starts to exceed the rate of weak interactions, causing the neutrinos to begin decoupling from the plasma. Still later, the process of $e^\pm$ annihilation releases entropy to the photons, increasing their temperature relative to the neutrinos. In fact, $T_\nu = T_\gamma \cdot (4/11)^{1/3}$ provided the neutrino decoupling is complete by the annihilation era. Since this is not quite true and to account for any hypothetical 'extra radiation species' (er), one introduces the *effective number of relativistic species* $N_{\rm eff}$ and writes instead

$$\rho_\nu + \rho_{\rm er} \equiv \frac{\pi^2}{15} T_\nu^4 \cdot \frac{7}{8} N_{\rm eff}. \tag{7.6}$$

Altogether, the radiation density can be written as

$$\rho_r = \rho_\gamma \left[1 + \frac{7}{8} \left(\frac{4}{11} \right)^{4/3} N_{\rm eff} \right]. \tag{7.7}$$

Finally, modern experiments have probed with increasing precision the CMB radiation density, which reveals conditions at the epoch of photon decoupling (redshift $z \simeq 1090$). Because of its contribution to ρ_r, $N_{\rm eff}$ affects various properties of the CMB [Hi *et al*. (WMAP collab.) 13], among them the peak locations of the baryon acoustic oscillations (BAO). The current fit with minimum uncertainty is found from combining data from BAO and CMB measurements [Ad *et al.* (Planck collab.) 13],

$$N_{\rm eff} = 3.30 \pm 0.27, \tag{7.8}$$

consistent with the Standard Model determination $N_{\rm eff} = 3.046$ [MaMPPPS 05].

https://doi.org/10.1017/9781009291033.007 Published online by Cambridge University Press

Problems

(1) **Three-generation neutrino mixing**

In three-generation mixing, the flavor ($\alpha = e, \nu, \tau$) and energy ($j = 1, 2, 3$) eigenstates are related by $|\nu_\alpha\rangle = U^*_{\alpha j}|\nu_j\rangle = U^\dagger_{j\alpha}|\nu_j\rangle$, as in Eq. (3.1).

(a) Show that the amplitude connecting initial and final flavor states $|\nu_\alpha\rangle$ and $|\nu_\beta\rangle$ is $\mathcal{A}_{\alpha\beta} = U_{\beta j}\mathcal{D}_j U^\dagger_{j\alpha}$, given that $\mathcal{D}$ is a phase factor (temporarily unspecified) describing the neutrino's propagation.

(b) Show that the transition probability is $\mathcal{P}_{\alpha\beta} = |\mathcal{A}_{\alpha\beta}|^2$ is expressible as

$$\mathcal{P}_{\alpha\beta} = \sum_{j=1}^{3} |U_{\beta j}|^2 |U_{\alpha j}|^2 + 2\sum_{j>k} U_{\beta j}U^*_{\beta k}U_{\alpha k}U^*_{\alpha j}\mathcal{D}_j\mathcal{D}^*_k.$$

Hint: Partition the double sum as $\sum_{j,k=1}^{3} = \sum_{j=1}^{3} + 2\sum_{j>k}$.

(c) Determine $\sum_{\beta=1}^{3} \mathcal{P}_{\alpha\beta}$.

(d) Assume that the neutrino propagation factor can be expressed as $\mathcal{D}_j\mathcal{D}^*_k = e^{-i\Delta m^2_{kj}L/2E}$, where L is the source-detector separation, E is the (relativistic) neutrino energy and, as in the text, $\Delta m^2_{kj} \equiv m^2_k - m^2_j$. Then show

$$\mathcal{P}_{\alpha\beta} = \sum_{j=1}^{3} |U_{\beta j}|^2 |U_{\alpha j}|^2 + 2\sum_{j>k} \cos\left[\frac{\Delta m^2_{kj}}{2E}L - \varphi_{\beta,\alpha;j,k}\right] |U_{\beta j}U^*_{\beta k}U_{\alpha k}U^*_{\alpha j}|,$$

where $\varphi_{\beta,\alpha;j,k}$ is the (*CP*-violating phase) of the U_{jk} factors.

(2) **Two-generation 1 $\leftrightarrow$ 3 neutrino mixing**

The aim is to obtain a simple expression for the survival probability $\mathcal{P}_{ee}(L)$ for $1 \leftrightarrow 3$ oscillations starting from the general relation derived above. We shall ignore *CP*-violating effects (and thus set $\varphi_{\beta,\alpha;j,k} = 0$) and use $|\Delta m^2_{21}| \ll |\Delta m^2_{31}| \simeq |\Delta m^2_{32}|$, which is already known from the text. Because we wish to observe $1 \leftrightarrow 3$ oscillations, we take $|\Delta m^2_{31}|L/2E \geq 1$ (i.e. $2\pi L/L^{(31)}_{\rm osc} \geq 1$). We also take $\Delta m^2_{21}L/2E \ll 1$ (i.e. $2\pi L/L^{(21)}_{\rm osc} \ll 1$) to suppress $1 \leftrightarrow 2$ oscillations. Then show that the survival probability $\mathcal{P}_{ee}(L)$ can be written as

$$\mathcal{P}_{ee}(L) = 1 - 2|U_{e3}|^2\left(1 - |U_{e3}|^2\right)\left(1 - \cos(2\pi L/L^{(31)}_{\rm osc})\right).$$

Hint: You will want to make use of the unitarity property of the mixing matrix U.

https://doi.org/10.1017/9781009291033.007 Published online by Cambridge University Press